Physics Letters B 774 (2017) 130–134

Contents lists available at ScienceDirect

Physics Letters B

www.elsevier.com/locate/physletb

Absorption of electromagnetic and gravitational waves by Kerr black holes

Luiz C.S. Leite [a,b], Sam R. Dolan [b,*], Luís C.B. Crispino [a]

[a] Faculdade de Física, Universidade Federal do Pará, 66075-110, Belém, Pará, Brazil
[b] Consortium for Fundamental Physics, School of Mathematics and Statistics, University of Sheffield, Hicks Building, Hounsfield Road, Sheffield S3 7RH, United Kingdom

ARTICLE INFO

Article history:
Received 29 August 2017
Accepted 17 September 2017
Available online 25 September 2017
Editor: M. Trodden

ABSTRACT

We calculate the absorption cross section for planar waves incident upon Kerr black holes, and present a unified picture for scalar, electromagnetic and gravitational waves. We highlight the spin-helicity effect that arises from a coupling between the rotation of the black hole and the helicity of a circularly-polarized wave. For the case of on-axis incidence, we introduce an extended 'sinc approximation' to quantify the spin-helicity effect in the strong-field regime.

1. Introduction

Black holes, once dismissed as a mathematical artifact of Einstein's theory of general relativity (GR), have come to play a central role in modern astronomy and theoretical physics [1,2]. In astronomy, black holes provide a solution: in galaxy formation scenarios, in active galactic nuclei and in core-collapse supernovae, for instance. In theoretical physics, black holes pose a challenge: as spacetime curvature grows without bound in GR, the classical theory breaks down. Yet, novel quantum gravity effects apparently remain shrouded by a horizon endowed with generic thermodynamic properties [3].

Two recent advances in interferometry have opened new data channels on astrophysical black holes. In September 2015, LIGO detected the first gravitational-wave signal: a characteristic 'chirp' from a black hole binary merger [4]. Hundreds more chirps are anticipated over the next decade [5]. In April 2017, the Event Horizon Telescope (EHT) [6] – a global array of radio telescopes linked by very long baseline interferometry – observed the supermassive black hole candidates Sgr. A* and M87* at a resolution three orders of magnitude beyond that of the Hubble telescope [7]. Ultimately, the EHT will seek to study the black hole shadow itself [8–10], using techniques to surpass the diffraction limit [11].

These experimental advances motivate study of the interaction of electromagnetic waves (EWs) and gravitational waves (GWs) with black holes [12–14]. EWs and GWs propagating on curved spacetimes in vacuum share some traits. For example, both possess two independent (transverse) polarizations that are parallel-transported along null geodesics in the ray-optics limit. Yet there are key physical differences. GWs are tenuous, in the sense that they are not significantly attenuated or rescattered by matter sources. GWs are typically long-wavelength and polarized, because rotating quadrupoles (for example, binary systems or asymmetric neutron stars) predominantly emit circular-polarized waves at twice the rotational frequency [15]. For example, $\lambda \sim 10^{-3}$ m for EHT observations, whereas $\lambda \sim 10^{7}$ m for GW150914.

In this Letter we examine the absorption of a monochromatic planar wave of frequency ω incident upon a Kerr black hole of mass M and angular momentum J in vacuum. We calculate the absorption cross section σ_{abs}, i.e., the cross-sectional area of the black hole shadow [8–10] beyond the ray-optics approximation. For the first time, we present unifying results for scalar ($s = 0$), electromagnetic ($s = 1$) and gravitational ($s = 2$) waves. Our results highlight the influence of two key phenomena: superradiance and the spin-helicity effect, described below.

The absorption scenario, illustrated in Fig. 1, is encapsulated by several dimensionless parameters: the ratio of the gravitational length to the (reduced) wavelength $GM\omega/c^3$; the dimensionless black hole spin $a^* \equiv a/M$ where $a = Jc^2/GM$ ($0 \le a^* < 1$); the spin of the field $s = 0, 1, 2$; the angle of incidence with respect to the black hole axis γ; and the helicity of the circular polarization ± 1. We adopt natural units such that $G = c = 1$.

* Corresponding author.
E-mail address: s.dolan@sheffield.ac.uk (S.R. Dolan).

https://doi.org/10.1016/j.physletb.2017.09.048

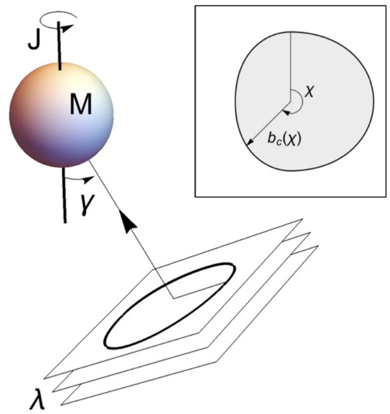

Fig. 1. A planar wave of frequency $\omega = 2\pi c/\lambda$ incident upon a rotating black hole of mass M and angular momentum J at an angle γ. *Inset:* the locus $b_c(\chi)$ of the black hole shadow on the wavefront.

2. Concepts

2.1. Black hole shadows

An observer studying a black hole in vacuum with a pinhole camera will see a dark region on the image plane defined by the set of null-geodesic rays entering the pinhole which, when traced backwards in time, pass into the black hole. The boundary of the shadow is determined by those rays which asymptote towards an (unstable) photon orbit, defining an angular radius $\alpha(\chi)$ in terms of the projection angle χ. Alternatively, a shadow can be defined on a planar surface in terms of an impact parameter $b(\chi)$, using those rays orthogonal the surface, as shown in Fig. 1. Far from the black hole, there is an approximately linear relationship $b(\chi) = r_0\alpha(\chi) + O\left(\frac{GM}{c^2 r_0}\right)$; the two approaches are closely related. Here we extend the latter approach to consider monochromatic waves of a finite wavelength.

In the geometrical-optics limit ($\lambda \to 0$), an observer at radial coordinate r_0 sees a shadow of angular radius α where [16]

$$\sin^2\alpha = \frac{27}{4}\frac{(\rho-1)}{\rho^3}, \qquad \rho \equiv \frac{r_0 c^2}{GM}. \tag{1}$$

For Sgr A*, $\alpha \approx 25$ µarcsec, with $r_0 \approx 8.3$ kpc and $M \approx 4.1 \times 10^6\ M_\odot$ [17]. In Kerr spacetime, α is a function of angle χ relative to the (projected) spin axis.

Here we seek to study Kerr shadows beyond the geometrical-optics regime. We shall focus on the difference between $\sigma_{\rm abs}(\omega)$, the absorption cross section at fixed frequency ω, and the $\sigma_{\rm geo}$, the geometric cross section defined by

$$\sigma_{\rm geo} = \tfrac{1}{2}\int_0^{2\pi} b_c^2(\chi)d\chi. \tag{2}$$

2.2. Superradiance and spin-helicity

Superradiance is a radiation-enhancement mechanism by which a black hole may shed mass and angular momentum and yet still increase its horizon area, and thus its entropy [18]. As a consequence, $\sigma_{\rm abs}$ may become negative at low frequencies, through stimulated emission. The effect is strongly enhanced by spin s.

The spin-helicity effect is a coupling between a rotating source, such as a Kerr black hole, and the helicity of a polarized wave of finite wavelength λ [19]. A rotating spacetime distinguishes and separates waves of opposite helicity [20–22]. In the weak-field, rays are deflected through an angle $\zeta\Theta_E$, with $\Theta_E \equiv \frac{4GM}{c^2 b}$ the Einstein angle and $\zeta = 1 + \ldots$ an asymptotic series in which the spin-helicity effect is anticipated at $O\left(\frac{J\lambda}{Mcb^2}\right)$ [19]. In the strong-field, we anticipate that waves with a counter-rotating circular polarization are preferentially absorbed ($\sigma^-_{\rm abs} > \sigma^+_{\rm abs}$).

3. Method

3.1. Waves on the Kerr spacetime

The Kerr spacetime is described in Boyer–Lindquist coordinates $\{t, r, \theta, \phi\}$ by the line element

$$\begin{aligned} ds^2 = &-\frac{1}{\Sigma}(\Sigma - 2Mr)\,dt^2 - \frac{4Mar\sin^2\theta}{\Sigma}dt\,d\phi + \frac{\Sigma}{\Delta}dr^2 \\ &+ \Sigma d\theta^2 + \frac{(r^2+a^2)^2\sin^2\theta - \Delta a^2\sin^4\theta}{\Sigma}d\phi^2, \end{aligned} \tag{3}$$

where $\Sigma \equiv r^2 + a^2\cos^2\theta$, and $\Delta \equiv r^2 - 2Mr + a^2$. We focus on the $a^2 < M^2$ case of a rotating BH with two distinct horizons: an internal (Cauchy) horizon located at $r_- = M - \sqrt{M^2 - a^2}$ and an external (event) horizon at $r_+ = M + \sqrt{M^2 - a^2}$.

In the vicinity of a Kerr black hole, perturbing fields are described by a single master equation, first obtained by Teukolsky [23] using the Newman–Penrose formalism. In vacuum the master equation takes the form

$$\begin{aligned} &\left[\frac{(r^2+a^2)^2}{\Delta} - a^2\sin^2\theta\right]\frac{\partial^2\psi}{\partial t^2} + \frac{4Mar}{\Delta}\frac{\partial^2\psi}{\partial t\partial\phi} \\ &+ \left[\frac{a^2}{\Delta} - \frac{1}{\sin^2\theta}\right]\frac{\partial^2\psi}{\partial\phi^2} - \Delta^{-\mathfrak{s}}\frac{\partial}{\partial r}\left(\Delta^{\mathfrak{s}+1}\frac{\partial\phi}{\partial r}\right) \\ &- \frac{1}{\sin\theta}\frac{\partial}{\partial\theta}\left(\sin\theta\frac{\partial\psi}{\partial\theta}\right) + (\mathfrak{s}^2\cot^2\theta - \mathfrak{s})\psi \\ &- 2\mathfrak{s}\left[\frac{a(r-M)}{\Delta} + \frac{i\cos\theta}{\sin^2\theta}\right]\frac{\partial\psi}{\partial\phi} \\ &- 2\mathfrak{s}\left[\frac{M(r^2-a^2)}{\Delta} - r - ia\cos\theta\right]\frac{\partial\psi}{\partial t} = 0, \end{aligned} \tag{4}$$

where $\mathfrak{s}$ is the spin-weight of the field. We use $\mathfrak{s} = -s$ throughout, where $s = 0, 1, 2$ for scalar, electromagnetic and gravitational fields, respectively. One can separate variables in Eq. (4) using the standard ansatz

$$\psi_{\mathfrak{s}lm\omega}(t, r, \theta, \phi) = R_{\mathfrak{s}lm\omega}(r)S_{\mathfrak{s}lm\omega}(\theta)e^{-i(\omega t - m\phi)}, \tag{5}$$

to obtain angular and radial equations,

$$\frac{1}{\sin\theta}\frac{d}{d\theta}\left(\sin\theta\frac{dS_{\mathfrak{s}lm\omega}}{d\theta}\right) + U_{\mathfrak{s}lm\omega}(\theta)S_{\mathfrak{s}lm\omega} = 0, \tag{6}$$

$$\Delta^{-\mathfrak{s}}\frac{d}{dr}\left(\Delta^{\mathfrak{s}+1}\frac{dR_{\mathfrak{s}lm\omega}}{dr}\right) + V_{\mathfrak{s}lm\omega}(r)R_{\mathfrak{s}lm\omega} = 0, \tag{7}$$

where

$$\begin{aligned} U_{\mathfrak{s}lm\omega} &\equiv \lambda_{\mathfrak{s}lm\omega} + 2am\omega - 2a\omega\mathfrak{s}\cos\theta - \frac{(m + a\cos\theta)^2}{\sin^2\theta} + \mathfrak{s}, \\ V_{\mathfrak{s}lm\omega} &\equiv \frac{1}{\Delta}\left[K^2 - 2(r-M)K\right] - \lambda_{\mathfrak{s}lm\omega} + 4i\omega\mathfrak{s}r, \end{aligned} \tag{8}$$

and $K \equiv (r^2 + a^2)\omega - am$. The angular functions $S_{\mathfrak{s}lm\omega}(\theta)$ are known as spin-weighted spheroidal harmonics, and have as limiting cases the spheroidal harmonics ($\mathfrak{s} = 0$) and the spin-weighted spherical harmonics ($a\omega = 0$).

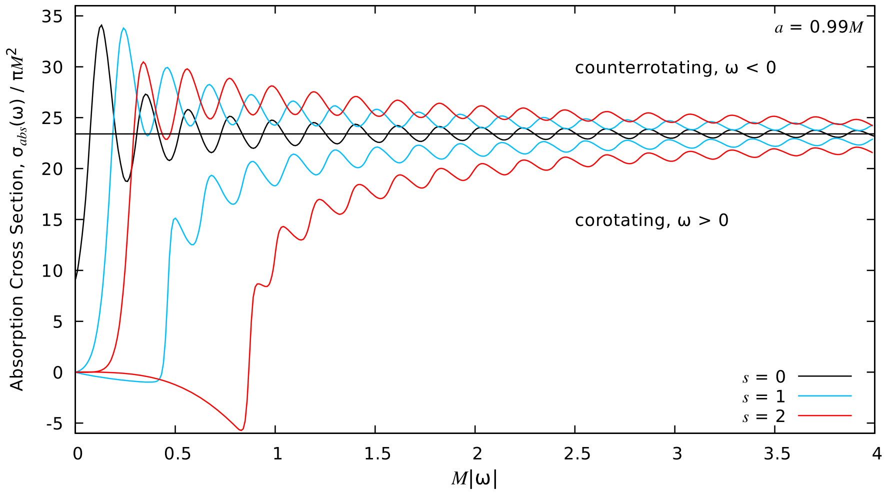

Fig. 2. The absorption cross section σ_{abs} for massless bosonic fields incident on a rapidly-rotating Kerr BH ($a = 0.99M$, $\gamma = 0$). For circularly-polarized fields ($s > 0$), the co-rotating ($\omega > 0$) and counter-rotating ($\omega < 0$) helicities are absorbed differently, due a coupling between the field helicity and the BH rotation.

We seek solutions of Eq. (7) that are purely ingoing at the event horizon, satisfying the following boundary conditions:

$$R_{\mathfrak{s}lm\omega} \sim \begin{cases} \mathcal{T}_{\mathfrak{s}lm\omega} e^{-\imath(\omega - m\Omega_h)r_\star} \Delta^{-\mathfrak{s}}, & r \to r_+, \\ \mathcal{I}_{\mathfrak{s}lm\omega} r^{-1} e^{-\imath\omega r_\star} + \mathcal{R}_{\mathfrak{s}lm\omega} r^{-(2\mathfrak{s}+1)} e^{\imath\omega r_\star}, & r \to +\infty, \end{cases} \tag{9}$$

where $\Omega_h \equiv \frac{a}{2Mr_+}$ is the angular frequency of the black hole horizon. Here $r_\star$ is the tortoise coordinate $r_\star \equiv \int dr \frac{(r^2+a^2)}{\Delta}$ such that $r_\star \to +\infty$ when $r \to +\infty$ and $r_\star \to -\infty$ when $r \to r_+$.

3.2. The absorption cross section

For an asymptotic incident plane wave traveling in the direction $\hat{n} = \sin\gamma\,\hat{x} + \cos\gamma\,\hat{z}$ the absorption cross section σ_{abs} is given by [24]

$$\sigma_{\mathrm{abs}} = \frac{4\pi^2}{\omega^2} \sum_{l=|\mathfrak{s}|}^{+\infty} \sum_{m=-l}^{+l} \left|S_{\mathfrak{s}lm\omega}(\gamma)\right|^2 \Gamma_{\mathfrak{s}lm\omega}. \tag{10}$$

The transmission factor $\Gamma_{\mathfrak{s}lm\omega}$ is the ratio of the energy passing into to the hole to that encroaching from infinity, $\frac{dE_{\mathrm{hole}}}{dE_{\mathrm{in}}}$ [18]. It takes the same sign as $\omega(\omega - m\Omega_h)$, so it is *negative* for low-frequency co-rotating modes. Using energy balance, $dE_{\mathrm{hole}} = dE_{\mathrm{in}} - dE_{\mathrm{out}}$, one obtains [24]

$$\Gamma_{0lm\omega} = 1 - \left|\frac{\mathcal{R}_{0lm\omega}}{\mathcal{I}_{0lm\omega}}\right|^2, \tag{11a}$$

$$\Gamma_{-1lm\omega} = 1 - \frac{B^2_{lm\omega}}{16\omega^4} \left|\frac{\mathcal{R}_{-1lm\omega}}{\mathcal{I}_{-1lm\omega}}\right|^2, \tag{11b}$$

$$\Gamma_{-2lm\omega} = 1 - \frac{\mathrm{Re}^2(C) + 144M^2\omega^2}{256\omega^8} \left|\frac{\mathcal{R}_{-2lm\omega}}{\mathcal{I}_{-2lm\omega}}\right|^2, \tag{11c}$$

for the scalar ($\mathfrak{s} = 0$), electromagnetic ($\mathfrak{s} = -1$), and gravitational ($\mathfrak{s} = -2$) cases, respectively. Here $B^2_{lm\omega} \equiv \lambda^2_{-1lm\omega} + 4am\omega - 4a^2\omega^2$, $\mathrm{Re}^2(C) = [(\lambda_{-2lm\omega} + 2)^2 + 4am\omega - 4(a\omega)^2](\lambda^2_{-2lm\omega} + 36am\omega - 36a^2\omega^2) + (2\lambda_{-2lm\omega} + 3)(96a^2\omega^2 - 48am\omega) - 144a^2\omega^2$, and $\mathcal{I}_{\mathfrak{s}lm\omega}$, $\mathcal{R}_{\mathfrak{s}lm\omega}$ are the coefficients appearing in the ingoing solutions of Eq. (9).

3.3. Numerical method

In order to determine the absorption cross section via Eq. (10) we first computed the spin-weighted spheroidal harmonics $S_{\mathfrak{s}lm\omega}$ and the transmission factors $\Gamma_{\mathfrak{s}lm\omega}$ by solving Eqs. (6) and (7) with numerical methods.

We obtained the spin-weighted spheroidal harmonics $S_{\mathfrak{s}lm\omega}$ and its corresponding eigenvalues $\lambda_{\mathfrak{s}lm\omega}$ using the *spectral eigenvalue method* as described in Ref. [13,25]. We have tested the angular eigenvalues $\lambda_{\mathfrak{s}lm\omega}$ obtained via the spectral eigenvalue method against the low-$a\omega$ formula provided in Ref. [26], obtaining a satisfying concordance.

The transmission factors were obtained as follows: in the scalar case ($\mathfrak{s} = 0$), we rewrote the radial equation into a Schrödinger-like form and numerically integrated it using the scheme detailed in Ref. [14]; in the electromagnetic ($\mathfrak{s} = -1$) and gravitational ($\mathfrak{s} = -2$) cases, we rewrote the radial Teukolsky equation using the *Detweiler* [27] and *Sasaki–Nakamura* [28] transformations, respectively. We numerically integrated the Detweiler and Sasaki–Nakamura equations from $r = r_h$ to $r = r_\infty$, where $r_h \sim 1.001r_+$ and $r_\infty \sim 10^3 r_+$ are within the near-horizon and the far-field regimes, respectively. At $r = r_\infty$, we extract the values of the ingoing and outgoing coefficients via (9) and compute the transmission factors via (11). To assure the reliability of our results, we have checked them using independent codes [13].

4. Results

4.1. Absorption cross sections

Fig. 2 shows the absorption cross section σ_{abs} for planar waves in all massless bosonic fields ($s = 0$, 1 and 2) impinging upon a rapidly-rotating Kerr BH ($a^* = 0.99$) parallel to the rotation axis ($\gamma = 0$). At long wavelengths, the incident wave stimulates superradiant emission from the black hole [29], with transmission turning negative for modes satisfying $\omega(\omega - m\Omega_h) < 0$. For on-axis incidence $\gamma = 0$, only the $m = -\mathfrak{s}$ modes contribute to the mode sum (10). Thus, σ_{abs} is negative for polarized fields ($s > 0$), but not for the scalar field ($s = 0$). The superradiant effect occurs principally in the $l = m = -\mathfrak{s}$ mode, and is much stronger for gravitational waves than for electromagnetic waves.

The absorption cross section for the co- and counter-rotating helicities are quite distinct, with the latter ($\omega < 0$) more strongly absorbed than the former ($\omega > 0$). This is a clear manifestation of

Table 1
The impact parameter b_c, orbital frequency Ω_c and Lyapunov exponent Λ_c for circular polar null geodesics, to 4 decimal places. See Eq. (13).

a^*	0	0.5	0.8	0.99	1
b_c/M	$\sqrt{27}$	5.1205	4.9849	4.8383	4.8284
$\Omega_c M$	$\frac{1}{\sqrt{27}}$	0.1958	0.2019	0.2089	0.2094
$\Lambda_c M$	$\frac{1}{\sqrt{27}}$	0.1884	0.1788	0.1633	0.1620

the spin-helicity effect for electromagnetic and gravitational waves. In the limit $M|\omega| \to \infty$, the difference falls off at $O(M|\omega|)^{-1}$ and $\sigma_{\rm abs}$ approaches the geodesic capture cross section $\sigma_{\rm geo}$. We now attempt to quantify this effect.

4.2. High frequency model

Fig. 2 exhibits regular oscillations in $\sigma_{\rm abs}(\omega)$ arising from successive l modes in Eq. (10). For scalar fields it was previously shown [30,14] that such oscillations are linked to the Regge pole spectrum of the black hole, whose asymptotic properties are set by the angular frequency Ω_c and Lyapunov exponent Λ_c of the circular photon orbits of the spacetime. At high frequencies for $\gamma = 0$, we find that $\sigma_{\rm abs}$ is well described by the *sinc approximation* [31,30,14],

$$\sigma_{\rm abs} \approx \sigma_{\rm sinc} \equiv \mathcal{C}_s + \varepsilon \mathcal{A}_s \sin\left(\mathcal{B}_s/\varepsilon\right), \tag{12}$$

where $\varepsilon \equiv (M|\omega|)^{-1}$ and $\{\mathcal{A}_s, \mathcal{B}_s, \mathcal{C}_s\}$ are spin-dependent terms to be described more fully below.

A sinc approximation of this form was first developed by Sanchez [31] in 1977, for scalar fields on the Schwarzschild spacetime. For the Kerr spacetime with a scalar field incident along the axis ($\gamma = 0$), it was shown in Ref. [14] (based on the method of Ref. [30]) that Eq. (12) that remains valid with

$$\mathcal{A}_0 = -\frac{4\pi\Lambda_c e^{-\pi\Lambda_c/\Omega_c}}{\Omega_c^2}, \qquad \mathcal{B}_0 = \frac{2\pi}{M\Omega_c}, \tag{13}$$

and $\mathcal{C}_0 = \sigma_{\rm geo} = \pi b_c^2$. Sample values for b_c, Ω_c and Λ_c are given in Table 1. The method for obtaining these values is covered in Ref. [14].

For $s > 0$, we now propose an extended model to include terms at $O(\varepsilon)$:

$$\mathcal{A}_{s>0} = \mathcal{A}_0, \tag{14a}$$

$$\mathcal{B}_{s>0} = \mathcal{B}_0\left[1 + \varepsilon\left(\bar{b}_s \pm s\, a^* \Delta b_s\right) + O(\varepsilon^2)\right], \tag{14b}$$

$$\mathcal{C}_{s>0} = \mathcal{C}_0\left[1 + \varepsilon\left(\bar{c}_s \pm s\, a^* \Delta c_s\right) + O(\varepsilon^2)\right]. \tag{14c}$$

The coefficients Δb_s and Δc_s encapsulate the effect of the spin-helicity interaction, with + in Eq. (14) for the co-rotating helicity, and − for the counter-rotating helicity. To find the coefficients we fitted the model to our numerical data $\sigma_{\rm abs}$ across the domain $M|\omega| \in [2.5, 4]$ for $0 \le a^* \le 0.99$. Fig. 3 shows that the model (12)–(14) fits the data well across the domain in ω.

We may draw several inferences from the best-fit parameter values shown in Fig. 3(c). First, that $\Delta b_1 = \Delta b_2$ and $\Delta c_1 = \Delta c_2$ to within the fitting error. This implies that the spin-helicity effect for gravitational waves is twice as large as for electromagnetic waves, as expected. Second, that $\mathcal{C}_s \Delta b_s < 0$, so counter-rotating helicities are preferentially absorbed. Third, that $\Delta c_s \to \Delta b_s$ as $a^* \to 0$, which was not anticipated *a priori*. Fourth, that $\mathcal{B}_0 \Delta b_s s a^*$, the spin-helicity part of the phase term in the sinc approximation (12), varies monotonically from 0 in the Schwarzschild case up to approximately $s\pi$ in the extremal limit ($a \to M$). Evidence of this phase shift can be seen in Fig. 3(a).

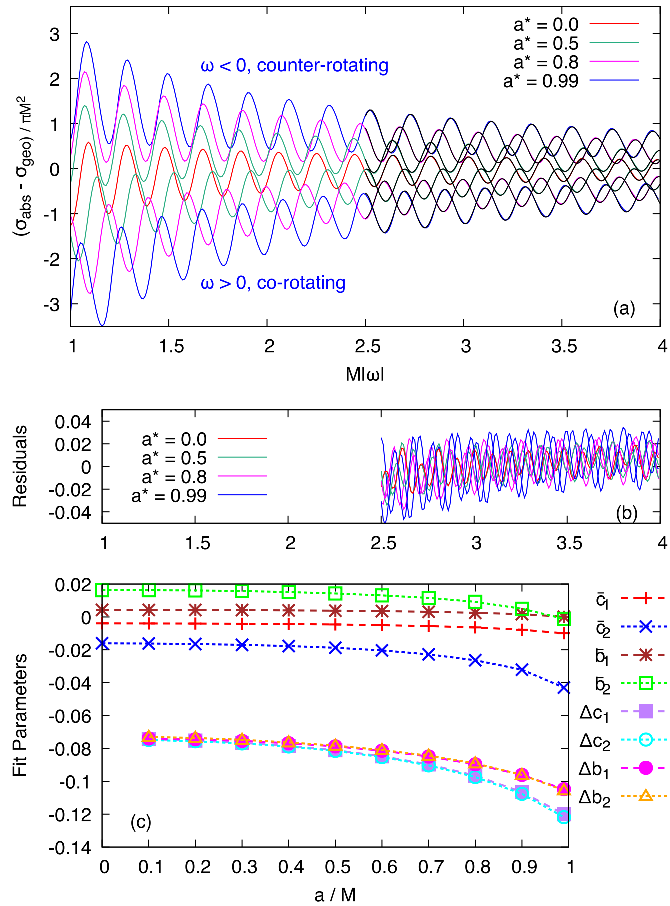

Fig. 3. (a) Fitting the sinc approximation model (12)–(14) to numerical data for $a^* \in \{0, 0.5, 0.8, 0.99\}$ across the domain $M|\omega| \in [2.5, 4]$. (b) The residuals of the fit, $|\sigma_{\rm abs} - \sigma_{\rm sinc}|/\pi M^2$. (c) The best-fit values for the parameters $\{\bar{c}_s, \bar{b}_s, \Delta c_s, \Delta b_s\}$ in Eq. (14).

5. Final remarks

We have calculated the absorption cross section for scalar, electromagnetic, and gravitational massless plane waves impinging upon a Kerr BH along its rotation axis. For the first time, we have presented a unified picture of the absorption spectrum for all the bosonic fields. We showed that superradiance leads to stimulated emission, rather than absorption, at low frequencies for co-rotating circular polarizations; and that counter-rotating polarizations are more heavily absorbed in general. We have proposed and tested an extended version of the sinc approximation, to encapsulate the spin-helicity effect at short wavelengths, where its effect falls off with λ/M.

An open question is whether the spin-helicity effect shown here can be quantitatively described using *spinoptics* [20–22]. That is, can a modified geometric-optics approximation, incorporating next-to-leading order helicity-dependent corrections in the eikonal equations, successfully reproduce the $1/M|\omega|$ terms in Eqs. (14)? Future work in this direction could prove illuminating.

Acknowledgements

The authors would like to thank Conselho Nacional de Desenvolvimento Científico e Tecnológico (CNPq) and Coordenação de Aperfeiçoamento de Pessoal de Nível Superior (CAPES), in Brazil, for partial financial support. S.D. acknowledges financial support from the Engineering and Physical Sciences Research Council

(EPSRC) under Grant No. EP/M025802/1 and from the Science and Technology Facilities Council (STFC) under Grant No. ST/L000520/1.

References

[1] K.S. Thorne, R.H. Price, D.A. MacDonald, Black Holes: The Membrane Paradigm, Yale University Press, 1986.

[2] V.P. Frolov, I.D. Novikov (Eds.), Black Hole Physics: Basic Concepts and New Developments, 1998.

[3] R.M. Wald, The thermodynamics of black holes, Living Rev. Relativ. 4 (2001) 6, http://dx.doi.org/10.12942/lrr-2001-6, arXiv:gr-qc/9912119.

[4] B.P. Abbott, et al., Observation of gravitational waves from a binary black hole merger, Phys. Rev. Lett. 116 (6) (2016) 061102, http://dx.doi.org/10.1103/PhysRevLett.116.061102, arXiv:1602.03837.

[5] B.P. Abbott, et al., Binary black hole mergers in the first advanced LIGO observing run, Phys. Rev. X 6 (4) (2016) 041015, http://dx.doi.org/10.1103/PhysRevX.6.041015, arXiv:1606.04856.

[6] A. Ricarte, J. Dexter, The Event Horizon Telescope: exploring strong gravity and accretion physics, Mon. Not. R. Astron. Soc. 446 (2015) 1973–1987, http://dx.doi.org/10.1093/mnras/stu2128, arXiv:1410.2899.

[7] D. Castelvecchi, How to hunt for a black hole with a telescope the size of Earth, Nature 543 (2017) 478–480.

[8] H. Falcke, F. Melia, E. Agol, Viewing the shadow of the black hole at the galactic center, Astrophys. J. 528 (2000) L13, http://dx.doi.org/10.1086/312423, arXiv:astro-ph/9912263.

[9] R.-S. Lu, A.E. Broderick, F. Baron, J.D. Monnier, V.L. Fish, S.S. Doeleman, V. Pankratius, Imaging the supermassive black hole shadow and jet base of M87 with the Event Horizon Telescope, Astrophys. J. 788 (2014) 120, http://dx.doi.org/10.1088/0004-637X/788/2/120, arXiv:1404.7095.

[10] T. Johannsen, Testing the no-hair theorem with observations of black holes in the electromagnetic spectrum, Class. Quantum Gravity 33 (12) (2016) 124001, http://dx.doi.org/10.1088/0264-9381/33/12/124001, arXiv:1602.07694.

[11] K. Akiyama, et al., Imaging the Schwarzschild-radius-scale structure of M87 with the Event Horizon Telescope using sparse modeling, Astrophys. J. 838 (1) (2017) 1, http://dx.doi.org/10.3847/1538-4357/aa6305, arXiv:1702.07361.

[12] K. Glampedakis, N. Andersson, Scattering of scalar waves by rotating black holes, Class. Quantum Gravity 18 (2001) 1939–1966, http://dx.doi.org/10.1088/0264-9381/18/10/309, arXiv:gr-qc/0102100.

[13] S.R. Dolan, Scattering and absorption of gravitational plane waves by rotating black holes, Class. Quantum Gravity 25 (2008) 235002, http://dx.doi.org/10.1088/0264-9381/25/23/235002, arXiv:0801.3805.

[14] C.F.B. Macedo, L.C.S. Leite, E.S. Oliveira, S.R. Dolan, L.C.B. Crispino, Phys. Rev. D 88 (2013) 064033, http://dx.doi.org/10.1103/PhysRevD.88.064033.

[15] B.P. Abbott, et al., The basic physics of the binary black hole merger GW150914, Ann. Phys. 529 (2017) 0209, http://dx.doi.org/10.1002/andp.201600209, arXiv:1608.01940.

[16] J.L. Synge, The escape of photons from gravitationally intense stars, Mon. Not. R. Astron. Soc. 131 (3) (1966) 463–466.

[17] A. Grenzebach, V. Perlick, C. Lämmerzahl, Photon regions and shadows of Kerr–Newman–NUT black holes with a cosmological constant, Phys. Rev. D 89 (12) (2014) 124004, http://dx.doi.org/10.1103/PhysRevD.89.124004, arXiv:1403.5234.

[18] R. Brito, V. Cardoso, P. Pani Superradiance, Lect. Notes Phys. 906 (2015) 1–237, http://dx.doi.org/10.1007/978-3-319-19000-6, arXiv:1501.06570.

[19] B. Mashhoon, Electromagnetic scattering from a black hole and the glory effect, Phys. Rev. D 10 (1974) 1059–1063, http://dx.doi.org/10.1103/PhysRevD.10.1059.

[20] V.P. Frolov, A.A. Shoom, Spinoptics in a stationary spacetime, Phys. Rev. D 84 (2011) 044026, http://dx.doi.org/10.1103/PhysRevD.84.044026, arXiv:1105.5629.

[21] V.P. Frolov, A.A. Shoom, Scattering of circularly polarized light by a rotating black hole, Phys. Rev. D 86 (2012) 024010, http://dx.doi.org/10.1103/PhysRevD.86.024010, arXiv:1205.4479.

[22] C.-M. Yoo, Notes on spinoptics in a stationary spacetime, Phys. Rev. D 86 (2012) 084005, http://dx.doi.org/10.1103/PhysRevD.86.084005, arXiv:1207.6833.

[23] S.A. Teukolsky, Rotating black holes: separable wave equations for gravitational and electromagnetic perturbations, Phys. Rev. Lett. 29 (16) (1972) 1114.

[24] J.A.H. Futterman, F.A. Handler, R.A. Matzner, Scattering from Black Holes, Cambridge University Press, 1988.

[25] G.B. Cook, M. Zalutskiy, Gravitational perturbations of the Kerr geometry: high-accuracy study, Phys. Rev. D 90 (12) (2014) 124021.

[26] E. Berti, V. Cardoso, M. Casals, Eigenvalues and eigenfunctions of spin-weighted spheroidal harmonics in four and higher dimensions, Phys. Rev. D 73 (2) (2006) 024013.

[27] S. Detweiler, On the Equations Governing the Electromagnetic Perturbations of the Kerr Black Hole, Proceedings of the Royal Society of London A: Mathematical, Physical and Engineering Sciences, vol. 349, The Royal Society, 1976, pp. 217–230.

[28] M. Sasaki, T. Nakamura, Gravitational radiation from a Kerr black hole. I. Formulation and a method for numerical analysis, Prog. Theor. Phys. 67 (6) (1982) 1788–1809.

[29] J.G. Rosa, Superradiance in the sky, Phys. Rev. D 95 (6) (2017) 064017, http://dx.doi.org/10.1103/PhysRevD.95.064017, arXiv:1612.01826.

[30] Y. Decanini, G. Esposito-Farese, A. Folacci, Universality of high-energy absorption cross sections for black holes, Phys. Rev. D 83 (2011) 044032, http://dx.doi.org/10.1103/PhysRevD.83.044032, arXiv:1101.0781.

[31] N.G. Sanchez, Absorption and emission spectra of a Schwarzschild black hole, Phys. Rev. D 18 (1978) 1030, http://dx.doi.org/10.1103/PhysRevD.18.1030.